

Computer Modeling Air Drawing in Melt Blowing Nonwovens

Process Produced by Dual Slot Annular Die

Bo ZHAO

¹College of Textiles, Zhongyuan University of Technology, Henan, Zhengzhou, 450007, P.R.China

ABSTRACT:

An air-drawing model of polymer melt blowing process is established and solved by introduced the numerical computation results of the air jet flow field of dual slot annular die. Meanwhile, the model is also verified by the experimental results obtained with our university's equipment. The influence of the density and the specific heat capacity of polymer melt at constant pressure changing with polymer temperature on the fiber diameter are also studied. The predicted fiber diameters tally with the experimental data well. The effects of the processing parameters on the fiber diameter are further investigated in this paper. We find that a lower polymer throughput rate, a higher polymer melt initial temperature, a higher air initial temperature, and a higher air initial velocity can all produce finer fibers. The results show the great perspective of this research in the field of computer-assisted design (CAD) of melt blowing process and technology.

KEYWORDS: *melt blowing, dual slot annular die, nonwovens, air drawing model, computer modeling, processing parameters, fiber diameter.*

I. INTRODUCTION

Melt blowing technology is a single step process to make melt blowing nonwovens directly from thermoplastic polymers with the aid of high velocity and hot air to attenuate the polymer melt fiber, which dates back to the 1950's [1]. The melt blowing web is ideally suited for medical materials, roof materials, hygienic materials, and so on. The dual slot annular die is shown in Figure 1. The annular die is often used to produce polymers fibers in this process. Researchers have been studying air drawing models of polymers, especially shambaugh and his colleagues [2-5].

In this paper, an air drawing model of polymer will be established based on numerical computational method and verify the numerical results with the experimental data obtained with our university's equipment, at the same time, we also consider the effects of the variation of polymer processing parameters and further study the effects of melt blowing process parameters on the fiber diameter. Based on the new air drawing model in melt blowing process, one improvement will be further made on the model in this work: considering the influences on fiber diameter of the variation of the density and the specific heat capacity of polymer melt at constant pressure changing with polymer temperature. The final fiber diameter can then be predicted with the aid of this air drawing model. It is found that the model can be applied to predicting the drawing effects successfully. Effects of the processing parameters on the fiber diameter will also be investigated by utilizing the

air drawing model. The results also reveal the great potential for this research in the computer-assisted design (CAD) of melt blowing process, technology and equipment.

II. AIR DRAWING MODEL OF POLYMERS IN MELT BLOWING PROCESS

The polymer air drawing model consists of a continuity equation, a momentum equation, an energy equation, and a constitutive equation [1, 6]. The surrounding air conditions (velocity and temperature) are considered as given functions of axial position, are obtained by numerical simulation. In the literatures [1-5], the density ρ_f and specific heat capacity of polymer melt at constant pressure C_{pf} are considered to be constant. In fact, they vary with polymer temperature T . In this research, we establish an air drawing model that differs from others in citations as indicated above, and consider the effects of the variation of polymer density and polymer specific heat capacity with polymer temperature at constant temperature. Because the air velocity and temperature obtained by the numerical solution of the air jet flow field of dual slot annular die, we can predict the drawing effects with the aid of this air drawing model.

2.1 Continuity equation

$$W = \frac{\pi}{4} D^2 V \rho_f \quad (1)$$

Where W =polymer mass flow rate, D =fiber diameter, V =fiber velocity, and ρ_f =polymer density. As the polymer density varies with polymer temperature, the following correlation [7] is also introduced:

$$\rho_f = \frac{1}{1.145 + 0.000903 \times T} \quad (2)$$

Where T is the polymer temperature.

2.2 Momentum equation

$$\frac{dF_{rheo}}{dz} = \frac{\pi}{2} j \rho_a C_f (V_a - V)^2 D + W \frac{dV}{dz} - \rho_f \frac{\pi}{4} D^2 g \quad (3)$$

Where F_{rheo} =rheological force, z =axial direction, ρ_a =air density, ρ_f =polymer density, V =fiber velocity, V_a =air velocity, g =gravitational acceleration, and C_f =air drawing coefficient.

The rheological force is as following.

$$F_{rheo} = \frac{\pi}{4} D^2 (\tau_{xx} - \tau_{yy}) \quad (4)$$

Where τ_{xx} = the axial tensile stress of polymer, and τ_{yy} =the transversal tensile stress of polymer.

C_f is given by the following correlation:

$$C_f = \beta \text{Re}^{-n} \quad (5)$$

β and n are the constants of Matsui's correlation and Re is the Reynolds number. Re is defined by the following relation:

$$Re = \frac{D |u_a - u|}{\nu_a} \quad (6)$$

Where ν_a =the air kinematic viscosity.

2.3 Energy equation

$$\rho_f C_{pf} \frac{dT}{dz} V = - \frac{4h(T - T_a)}{D} \quad (7)$$

Where T =polymer temperature, T_a =air temperature, h =heat transfer coefficient, C_{pf} =specific heat capacity of the polymer at constant pressure, and C_{pf} =specific heat capacity of the polymer at constant pressure.

Like polymer density, the correlation of the specific heat capacity at a constant pressure of the polymer melt changing with the polymer temperature [7] is as following:

$$C_{pf} = 0.3669 + 0.00242 \times T \quad (8)$$

2.4 Constitutive equation

As is commonly known, polypropylene polymer is a kind of non-Newtonian fluid, the constitutive equation of a power-law fluid is introduced in our model.

$$\begin{aligned} \tau_{xx} &= 2\eta \left(\frac{dV}{dz} \right)^m \\ \tau_{yy} &= -\eta \left(\frac{dV}{dz} \right)^m \end{aligned} \quad (9)$$

Where τ_{zz} =axial extra stress of polymer, τ_{xx} =transversal extra stress of polymer, η =shear viscosity, and m is power-law exponent.

2.5 Boundary conditions

$$V(0)=V_0, F(0)=F_0, D(0)=D_0, T(0)=T_0, F_{rheo}(0)=0 \quad (10)$$

Here F_0 =he initial rheological force of the polymer melt, V_0 =the initial velocity of the polymer melt, D_0 =initial diameter of the polymer melt, and T_0 =the initial temperature of the polymer melt .

The “freezing-point” is defined as the boundary condition. The method used for determining the initial rheological force F_0 is the searching “freezing-point” method, which requires checking whether the fiber diameters before and beyond some “point” along the filament are equal to each other when F_0 is considered to be the sum of the cumulative gravitational and air drawing force acting upon the frozen part of the filament fiber. If the fiber diameters are found to be the same, the “point” is the so-called “freezing-point” and used in this iteration is the appropriate initial rheological force

III. EXPERIMENTAL

3.1 Material characterization

The polymer used is Y-3500 polypropylene with a melt flow rate of 34.2g/10min.

3.2 Process parameters

The melt blowing processing parameters concerned are the polymer throughput rate, polymer melt initial temperature, air initial temperature, and air initial velocity and die-to-collector distance, the ranges of the parameters are 0.30-0.98g/min/hole, 275-330°C, 275-340°C, 30-145m/s and 0-25cm, respectively. To condense the discussions and comparison, a group of fundamental parameters was assumed during the computations: a polymer throughput rate 0.64 g/min/hole, a polymer melt primary temperature 300°C, a air initial velocity 85m/s, a air initial temperature 300°C and die-to-collector distance 18cm, When one of the processing parameters was varied, the fundamental values of the other process parameters were held constant.

3.3 The parameters of dual-slot annular die of melt blowing process

The dual slot annular die parameters are as following: The outside diameter $h=2.40\text{mm}$, the slot wide $e=0.56\text{mm}$, and the inside diameter $b=1.28\text{mm}$.

3.4 Test conditions

All the samples tested are conditioned for 24 hours at 65% RH and 20°C before evaluation.

3.5 Test methods

The image analysis method was employed to measure the fiber diameter. The images of nonwoven samples were acquired with a Questar three-dimensional video frequency microscope (Questar Corp., New Hope, PA) with an enlargement factor of 600 and a depth of focus of 1mm and then processed with Image-Pro Plus image analysis software(Media Cybernetics, Inc., Silver Spring, MD) to measure the fiber diameter. The image processing includes enhancement, smoothing, binarization, and filtering. The fibers of the melt blowing nonwoven are regarded as cylinders because their cross sections are nearly round. Twenty fibers are chosen to measure their diameters in each grid, so altogether there are 200 fibers to be measured in 10 grids. The mean value of the diameters of 200 fibers was considered as the fiber diameter of the polypropylene (PP) nonwoven sample.

The melt flow index (MFI) experiments of polypropylene (PP) were measured (performed) with a temperature 230°C, a load capacity 2.160kg, a aperture of capillary tube 2.095mm and a length of capillary tube 8mm on RL--11B type melt flow indexer at ambient room temperature conditions.

3.6 Numerical methods for solving the air jet flow field model of melt blowing

The air jet flow field model is solved by using the finite difference method. The SIMPLE algorithm is utilized to solve the problem of velocity pressure couple and the staggered grid is presented to avoid tooth-like distributions of velocity and pressure. The preferred difference scheme for space independent variables is the second-order upwind difference scheme and the TDMA method is used to solve the difference equations.

With the help of numerical simulations of the air jet flow field, we can determine the distributions of the x-component of air velocity V_a and air temperature T_a along the axial position x. Then we can solve the air drawing model of the polymer using a fourth-order Runge-Kutta method.

IV. EFFECTS OF VARIATIONS OF THE PROCESSING PARAMETERS ON THE FIBER DIAMETER

4.1 Effect of the polymer throughput rate on the fiber diameter

Figure 2 shows the effect of the polymer throughput rate on fiber diameter. The polymer throughput rate is 0.88, 0.64 and 0.48 g/min/hole in turn from top to bottom. As expected, lower polymer throughput rates give finer fibers and more rapid attenuation. When the polymer throughput rate is 0.48g/min/hole, the final fiber diameter is 19.1% finer than that when the polymer throughput rate is 0.88g/min/hole.

4.2 Effect of the polymer melt initial temperature on the fiber diameter

Figure 3 illustrates how changes in polymer melt initial temperature cause changes in the rate of fiber attenuation. The polymer melt initial temperature is 280, 300 and 320°C are considered. As expected, the higher polymers melt initial temperature, the finer the fibers will be. The fiber diameter corresponding to the polymer melt initial temperature of 320°C is 19.9% finer than that corresponding to the temperature of 280°C.

4.3 Effect of the air initial velocity on the fiber diameter

Figure 4 reveals the effect of the air initial velocity on fiber diameter. The air initial velocity is 50, 85, and 115m/s in turn from top to bottom. Note that the higher the air initial speed is, the finer the fibers will be. The higher air initial velocity will cause the fibers to be attenuated much higher. When the air initial speed increases to 115m/s, the final fiber diameter is 20.5% finer than that when the air initial speed is 50m/s.

4.4 Effect of the air initial temperature on the fiber diameter

Figure 5 shows the effect of the higher polymer melt initial temperature on fiber diameter. The air initial temperature is 280, 300, and 320°C in turn from top to bottom. As expected, higher polymer melt initial temperature will cause the fibers to be more finely attenuated. The fiber diameter corresponding to the polymer melt initial temperature of 320°C is 18.6% finer than that corresponding to the temperature of 280°C.

V. COMPARISON OF IMPROVED MODEL WITH PRIMARY MODEL

Model predictions considering the influences of the polymer temperature on the density and specific heat capacity of polymer melt at constant pressure. The melt blowing process parameters here are the polymer throughput rate, the polymer melt initial temperature, the air initial temperature, and the air initial velocity, and the variation ranges of the parameters are 0.30--0.98 g/min/hole, 275--330°C, 275--340°C, and 30-145m/s, respectively.

Table 1 shows the fiber diameter changing by considering the polymer density and the specific heat capacity of polymer melt at constant pressure varying with the polymer temperature. As can be seen, the predictions given by the two models are not same, two models have much difference from each other. It can be concluded that the variations in density and the specific heat capacity of polymer melt at constant pressure with the polymer temperature have very important effects on fiber diameter.

The model predictions can be improved remarkably by considering the influences of polymer temperature on the density and specific heat capacity of polymer melt at constant pressure. Therefore, the variation in density and specific heat capacity of polymer melt at constant pressure with the polymer temperature has important effects on fiber diameter. It has been concluded that the predicted fiber diameters are much closer to the experimental results, which further confirms the effectiveness of the polymer air drawing model established in this paper. From the above analyses, it can be seen that the fiber diameter is directly related to the polymer throughput rate, polymer melt initial temperature, air initial temperature, and air initial velocity.

VI. CONCLUSIONS

In this paper, an air drawing model of polymer will be established based on numerical computational method and verify the numerical results with the experimental data obtained with our university's equipment, at the same time, we also consider the effects of the variation of polymer processing parameters and further study the effects of melt blowing process parameters on the fiber diameter. The final fiber diameter can then be predicted with the aid of this air drawing model. It is found that the model can be applied to predicting the drawing effects successfully. Effects of the processing parameters on the fiber diameter will also be investigated by utilizing the air drawing model. The results also reveal the great potential for this research in the computer-assisted design (CAD) of melt blowing process, technology and equipment.

REFERENCES

- [1]. M. A. J. Uyttendaele, , *AICHE J.*, 36, 175 (1990)
- [2]. V. Bansal, and R. L. Shambaugh, *Ind. Eng. Chem. Res.*, 37, 1799 (1998)
- [3]. A. S. Harpham, and R. L. Shambaugh, *Ind. Eng. Chem. Res.*, 36, 3937 (1997)
- [4]. B. Majumdar, and R. L. Shambaugh, *J. Rheol.*, 34, 591(1990).
- [5]. A. S. Harpham, and R. L. Shambaugh, *Ind. Eng. Chem. Res.*, 35, 1099 (1996)
- [6]. T. Chen, *Textile Res. J.*, 73, 651(2003).
- [7]. K. F. Zieiminski, and J. E. Spruiell, *Synthetic Fibers*, 25, 31(1986).

ACKNOWLEDGEMENTS

The permission by Phoenix Inc. to use their software with an educational license is gratefully acknowledged.

NOMENCLATURE

W= polymer mass flow rate, kg/s.

D= filament fiber diameter, mm.

V= filament fiber velocity, m/s.

V_a = air velocity, m/s.

g= gravitational acceleration, g/s^2

C_{pf} =specific heat capacity of melt, J/(kg.K).

h=convective heat transfer coefficient, W/ (m².K)

T= polymer temperature, °C

T_a = the air temperature, °C

j = sign carrier of the air drag force, when j is -1 for $v_a > v$ and 1 for $v_a < v$.

Greek Symbols

ρ_f =polymer density, kg/m³.

ρ_a = air density, kg/m³.

η = the shear viscosity of air, Pa.s

τ_{zz} =axial extra stress, Pa.

τ_{xx} =transversal extra stress, Pa.

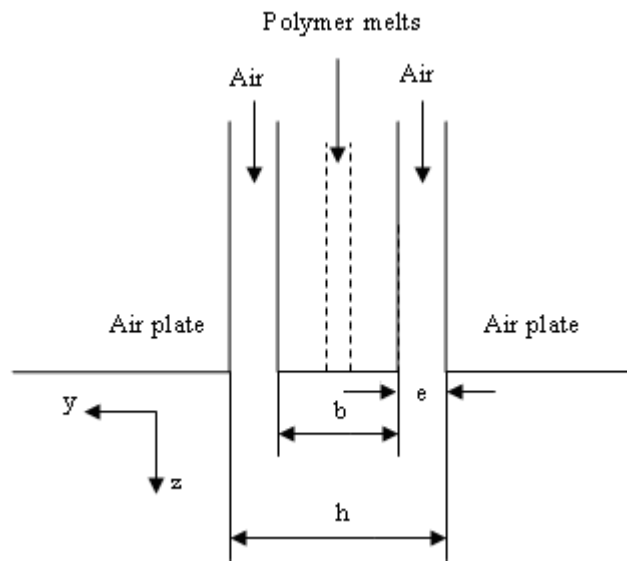


Fig.1. Dual-slot annular die of melt blowing process

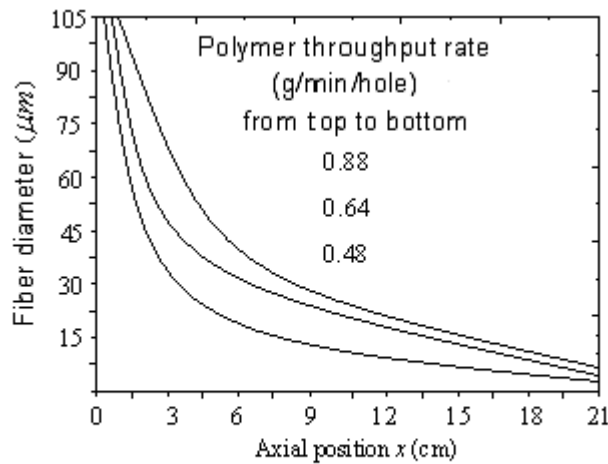


Fig. 2 Showing relationship between fiber diameter and axial position with polymer throughput rate (g/min/hole)

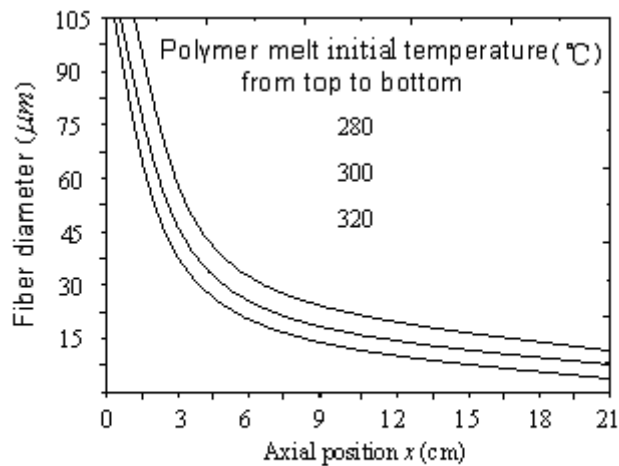


Fig. 3 Showing relationship between fiber diameter and axial position with polymer melt initial temperature (°C)

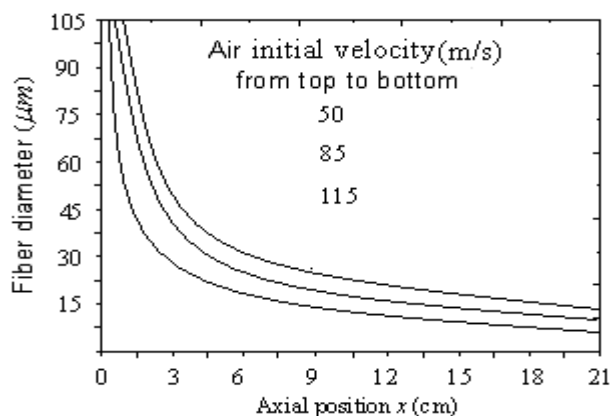


Fig. 4 Showing relationship between fiber diameter and axial position with air initial velocity(m/s)

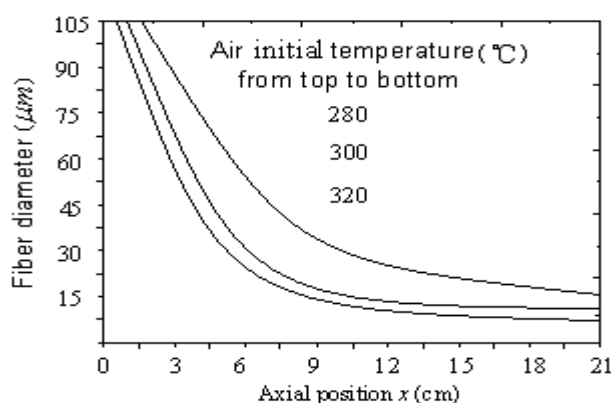


Fig. 5 Showing relationship between fiber diameter and axial position with air initial temperature (°C)

Table 1. Comparison of model predictions between improved model and primary model

Improved Model			Primary Model		
Measured diameter (μm)	Predicted diameter (μm)	Prediction error (%)	Measured diameter (μm)	Predicted diameter (μm)	Prediction error (%)
12.569	12.022	4.35	12.569	11.420	9.14
11.234	10.754	4.27	11.234	10.324	8.10
13.416	12.978	3.26	13.416	12.512	6.74
14.112	13.502	4.32	14.112	13.232	6.24
13.239	12.664	4.34	13.239	12.224	7.67

Corresponding author: Dr. Bo Zhao

Mailing Address: College of Textiles, Zhongyuan University of Technology, No.41 Zhongyuan Road, Zhengzhou, Henan 450007, People’s Republic of China